

Resistivity and lattice parameter variations in Nb₂Al type sigma phases

PAUL WENCIL BROWN*, F.J. WORZALA

Department of Materials Science, University of Wisconsin, Madison, Wisconsin, USA

The order dependencies of the resistance ratios and lattice parameter variations of Nb₂Al and Ta₂Al have been examined. These reflect the effects of composition variations across the single phase regions rather than those of classical order-disorder reactions. The nature of the order has also been observed to affect the dimensions of the tetragonal unit cells. This can be understood in terms of site ordering variations and can be in part attributed to the deviation from sphericity of atoms in certain crystallographic site types.

1. Introduction

Nb₂Al and Ta₂Al exist in the sigma phase structure, $D_{4h}^{14}-P4_2/mnm$, and are the only binary sigma phase compounds which contain a non-transitional element. The single phase region for Nb₂Al extends from about 32 to about 37 at.% Al [1]. That for Ta₂Al extends from about 20 to about 40 at.% Al

[2]. Since these single phase regions surround stoichiometric compositions at 33.3 at.% Al, they are generally referred to as Nb₂Al and Ta₂Al. Except when discussing a particular composition, this convention will be followed.

The sigma phase body centred tetragonal unit cell contains 30 atoms distributed among five non-equivalent crystallographic site types (Fig. 1, Table I).

The ordering schemes for stoichiometric material (Table II) place the transition metal atoms in the more highly co-ordinated B, C, and E sites and the Al atoms in the A and D sites. For compositions to the left of A₂B stoichiometry the transition metal atoms were observed to substitute randomly into the A and D sites. That is, the ratios of the number of transition metal atoms in the A and D sites to the number of A and D sites per cell are

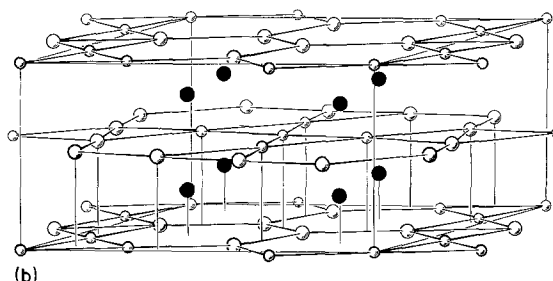
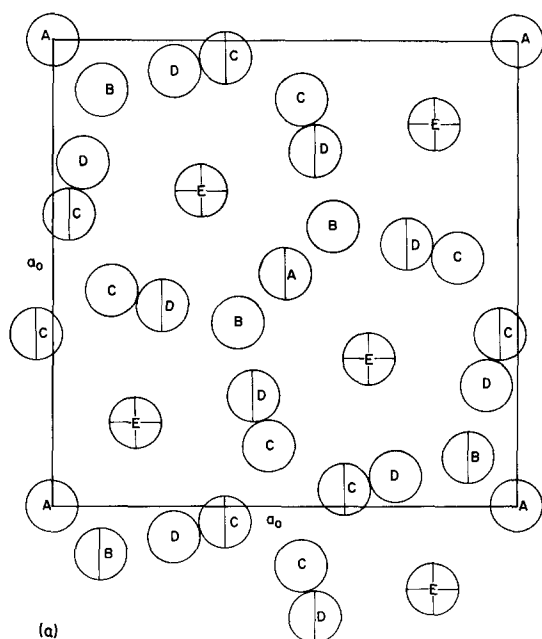


Figure 1(a) The sigma phase unit cell as viewed along the Z or [001] direction. The five crystallographic site types, A to E, are shown. The A sites define the body centred tetragonal structure and the E sites form closely packed linear atomic chains. Open circles indicate atoms at $Z = 0$ or 1, crossed circles atoms at about $Z = 1/4$ or $3/4$, and halved circles atoms at $Z = 1$. (b) A perspective view of the sigma phase unit cell from [31]. The E sites have been shaded.

* Present address: National Bureau of Standards, Washington, D.C., USA.

the same. For compositions to the right of stoichiometry, Al atoms initially substitute exclusively into the E sites in both systems until about one of the eight E sites per cell is occupied by an Al atom. Near this composition, 36.6 at.% Al, the rich Nb₂Al single phase boundary is reached. The Ta–Al sigma phase, however, is more stable and responds to this E site Al saturation by allowing C site Al substitution to begin. This continues as the Al rich Ta₂Al single phase boundary at about 40 at.% Al is reached. At this composition the structure contains 2 Al atoms per cell beyond the stoichiometric amount, one in the E sites and one in the C sites.

TABLE I

| Site type | Atoms/cell | Co-ordination number |
|-----------|------------|----------------------|
| A | 2 | 12 |
| B | 4 | 15 |
| C | 8 | 14 |
| D | 8 | 12 |
| E | 8 | 14 |

TABLE II

| Site type | Percentage occupation | |
|-----------|-----------------------|-----|
| | Nb or Ta | Al |
| A | 0 | 100 |
| B | 100 | 0 |
| C | 100 | 0 |
| D | 0 | 100 |
| E | 100 | 0 |

2. Experimental

Mixtures of the elemental powders were blended and compacted in the usual way. These were then sintered under high vacuum and arc-melted under a dynamic partial atmosphere of helium. After melting, Al-depleted surface areas were removed and the buttons wrapped in niobium foil and homogenized for 48 h at 1500°C. In most cases the homogenization anneal was followed by an ordering treatment of 240 h at 750°C. Both treatments were carried out under a vacuum of at least 5×10^{-7} Torr. Annealing weight losses were negligible. Once annealed, the samples were sectioned to their final dimensions of about 0.10 cm × 0.04 cm × 0.38 cm. The samples were then temporarily mounted in sealing wax contained by copper tubing and mechanically polished. Optical metallographic observations were conducted on the two major flats of each sample to determine the phases present and their distributions.

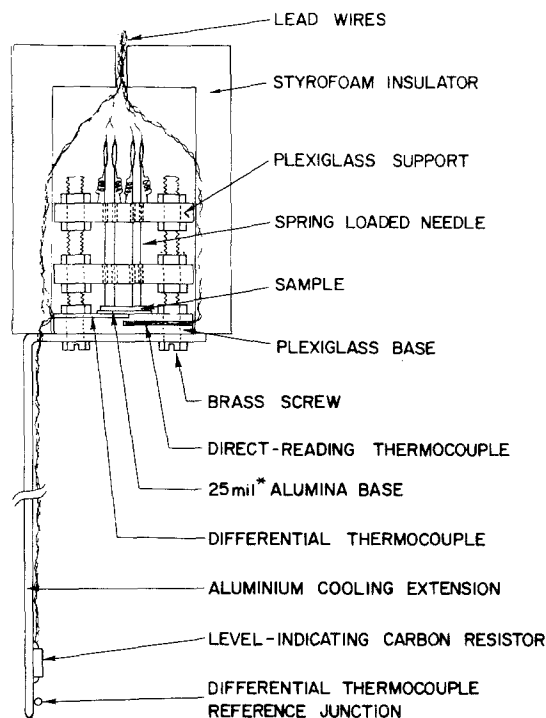


Figure 2 The four-point probe portion of the resistance measuring device.

* 1 mil = 2.5400×10^{-5} m.

Resistance determinations were carried out with a modified four-point probe device shown in Fig. 2. The geometry and brittleness of the samples required modification of the usual resistance measuring technique. The d.c. power supply was operated in a constant current mode and the voltage drop across the sample fed into a nonovolt amplifier and then into the Y-axis of an X–Y plotter. The output from one of two chromel versus gold 0.07 at.% iron thermocouples placed in the vicinity of the sample was fed into a millivolt amplifier and then into the X-axis of the X–Y plotter. A direct reading thermocouple was employed in the determination of the overall temperature–resistance curves between room temperature and 4.2 K. Cooling rates below about 30 K were 0.5 K min^{-1} or less. After the resistance measurements were carried out, the samples were crushed to $< 8 \mu\text{m}$ powders. Lattice parameter measurements were then made on these powders by diffractometry. Samples whose compositions spanned the Nb₂Al and Ta₂Al single phase regions and two phase samples containing small amounts of Ta₂Al₃, Nb₃Al or NbAl₃ were examined. Compositions were determined by three techniques: Al weight loss during arc melting, neutron activa-

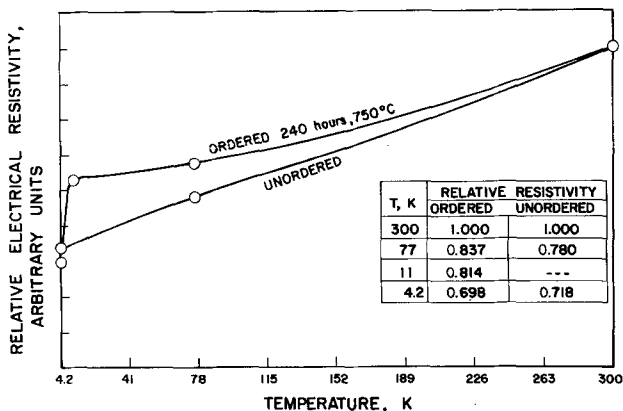


Figure 3 The variation in resistance with temperature in sample B before and after an ordering anneal.

Figure 4 The resistance variation with temperature in sample B after ordering for temperatures approaching 4.2° K.

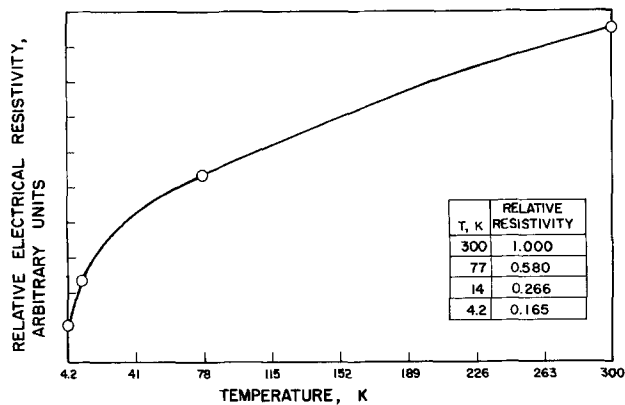
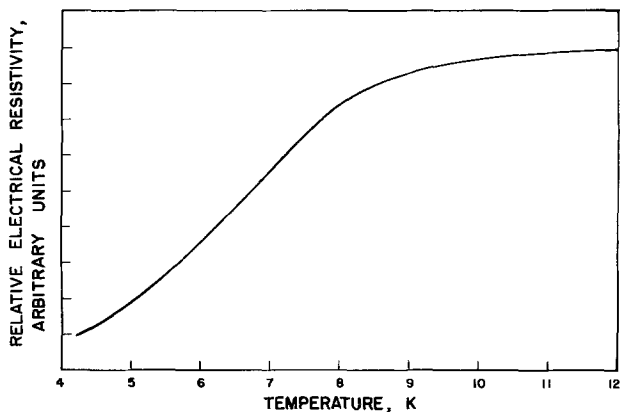


Figure 5 The variation of resistance with temperature in a nearly stoichiometric sample, D.

TABLE III

| Sample* | Composition (at. % Al) | $R(300)/R(4.2)$ | $a_0(\text{Å}) \pm 0.002$ | $c_0(\text{Å}) \pm 0.002$ |
|-----------|------------------------|-----------------|---------------------------|---------------------------|
| A | 31.5 ± 0.3 | Not measured | 9.957 | 5.116 |
| B: | | | | |
| ordered | 31.9 ± 0.2 | 1.43 | 9.954 | 5.167 |
| unordered | 31.9 ± 0.2 | 1.39 | 9.954 | 5.167 |
| C | 32.6 ± 0.5 | 1.73 | 9.950 | 5.164 |
| D | 33.4 ± 0.3 | 6.07 | 9.942 | 5.160 |
| E | 34.8 ± 0.3 | 1.55 | 9.931 | 5.173 |
| F | 37.5 ± 0.3 | 1.30 | 9.914 | 5.180 |

* Ordered for 240 h at 750° C unless otherwise noted.

tion analysis, and optical metallography. All were in excellent agreement.

3. Results

Table III lists the compositions, resistance ratios, and lattice parameters of the Nb–Al samples studied. The compositional uncertainties listed reflect the variances between the weight loss and activation analysis data. Figs. 3 and 4 show temperature–resistance curves for sample B whose composition lies almost exactly on the phase boundary between Nb₂Al and Nb₃Al. Metallographic examination indicated the sample to contain only a few tenths of a percent of Nb₃Al. Fig. 3 compares the resistance changes between room temperature and 4.2 K before and after an ordering treatment of 240 h at 750°C. The unannealed sample exhibited an almost linear decrease in resistance with temperature. The resistance of the ordered sample, however, did not decrease as rapidly until near 11 K. Below this temperature the resistance decreased rapidly resulting in a larger total resistance decrease in this case (Table III).

Initially, it was believed that this resistance decrease was the result of the onset of supercon-

ductivity in the Nb₃Al. However, a superconducting transition could not be observed inductively since the volume of Nb₃Al in the sample was too small and metallography revealed the presence of isolated Nb₃Al precipitates which did not exhibit a preference for grain boundaries. Thus the probability of an interconnected Nb₃Al second phase “shortening” the sample was quite low. This was further substantiated by carrying out critical temperature determinations on ordered and unordered two-phase samples whose composition was near 29 at. % Al. Both samples exhibited transition midpoints near 16.5 K and the Nb₃Al superconducting transitions were found to be complete at 16 K. This is about 5 K above the temperature at which the rapid resistance decrease in sample B was seen to initiate.

Fig. 5 is a temperature–resistance curve for sample D. The composition of this sample is very close to Nb₂Al stoichiometry. A rapid resistance decrease at low temperature may also be seen in this figure. However, the rapid decrease initiates about 20 K at this composition. Fig. 6 shows the temperature–resistance curve for sample F. The composition of this sample lies in the two-phase

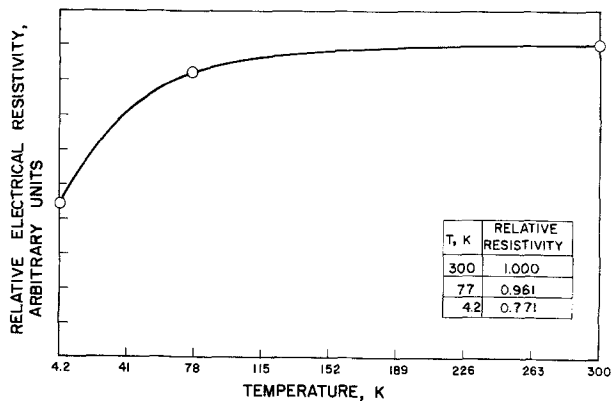
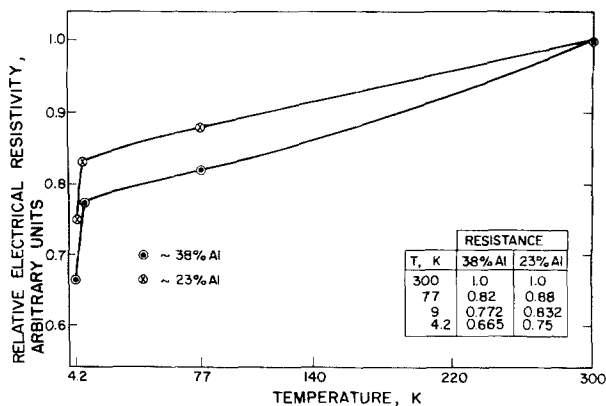


Figure 7 The variations in resistance with temperature of two Ta–Al sigma phase samples having substantially different compositions.

Figure 6 The variation of resistance with temperature in an Al-rich sample, F.



position has been drawn to exhibit a linear dependence in accord with Vegard's Law. Generally, the unit cell expands in the c_0 dimension with increasing Al content, although there is a contraction in the curve near Nb_2Al stoichiometry (Fig. 8c). This contraction parallels the increase in the resistance ratios. These effects appear to be order dependent since they occur only as the degree of compositionally dependent order approaches 100% as shown in Table II and is not unexpected considering the complexity of this structure.

The E sites which control the c_0 parameter, virtually independently of the a_0 parameter [8], are occupied exclusively by transition metal atoms at stoichiometry. In Nb_2Al the interatomic spacing in this direction is approximately $c_0/2$ or 2.58 Å. This compares with a distance of closest approach of about 2.86 Å in elemental Nb. As has been pointed out [8], these sites may be viewed as ellipsoidal rather than spherical. The contraction of the c_0 parameter in this structure would then be affected by the structural symmetries of the planes orthogonal to the direction of the E site chains, namely the populations of B, C and D crystallographic site types. The nature of the atomic species present in the body centred position would play no role in symmetry considerations. Since symmetry is maximized at stoichiometry, when the structure is fully ordered, a maximum E site expansion into its orthogonal directions would be allowed. As a consequence a contraction maximum in c_0 is observed at this point.

The parametric variation with composition across the Ta_2Al single phase region is shown in Fig. 9. Except for the sample with a composition near 35 at. % Al, error bars indicating a compositional uncertainty of 1% and a parametric uncertainty of 0.010 Å are shown. Since, unlike with Nb_2Al , it was not always possible to base the parametric calculations on the positions of the same reflections, these larger parametric uncertainties exist. However, the general shapes of the curves parallel those observed for Nb_2Al and can also be justified in terms of the observed site ordering schemes.

No contraction in the c_0 parameter was observed (Fig. 9b) since parametric measurements were not carried out on samples with compositions very close to stoichiometry. Samples whose compositions were close to stoichiometry tended to exhibit rather broad diffraction peaks over the angular range of interest. Since the atomic species

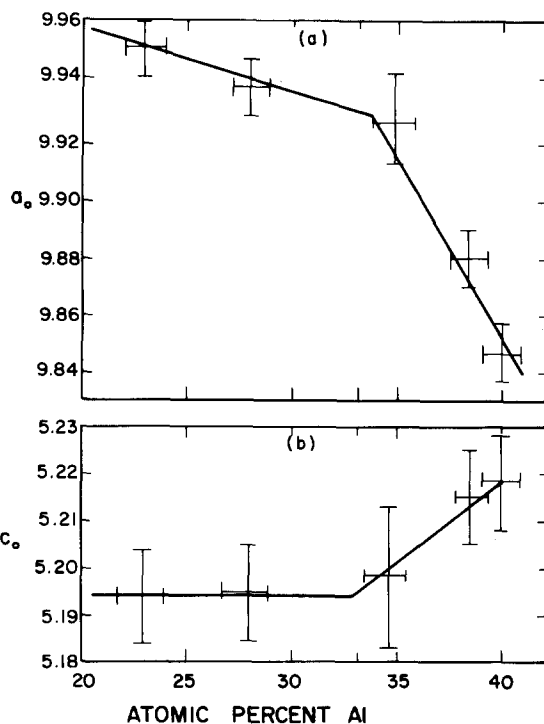


Figure 9 The variations in the a_0 lattice parameter (a) and the c_0 lattice parameter (b) with composition across the Ta_2Al phase region.

present in the E sites does not change for compositions to the left of stoichiometry, it follows that the c_0 parameter should remain relatively constant over this composition range. To the right of stoichiometry as Al atoms begin to substitute into E sites, the c_0 parameter begins to expand. Insufficient data exist to ascertain the precise effect of the initiation of C site Al atom substitution on this expansion.

The variation in the a_0 parameter with composition has also been approximated by two straight lines (Fig. 9a). These lines may be seen to intersect at a composition very close to stoichiometry. To the left of stoichiometry the random substitution of Ta for Al atoms in the A and D sites results in a slowly increasing a_0 parameter. This can be understood in terms of the replacement of the "smaller" Al atoms by the "larger" Ta atoms. At compositions to the right of stoichiometry the opposite occurs, Al atoms replace Ta atoms, and a_0 contracts. Similar behaviour is observed in the Nb-Al system. The contraction of the a_0 parameter in the Ta-Al system can be understood for compositions to the right of about 37 at. % Al as Al atoms C site substitution initiates. It is not clear why E site Al atom substitution result in an a_0 contraction

TABLE IV

| Sample* | Composition (at. % Al) | a_0 (Å) | c_0 (Å) |
|---------|---------------------------|-----------------|-----------------|
| 1 | 23.3 ± 1.0 | 9.95(0) ± 0.010 | 5.19(4) ± 0.010 |
| 2 | 28.0 ± 1.0 | 9.93(6) ± 0.010 | 5.19(5) ± 0.010 |
| 3 | 35.0 ± 1.0 | 9.92(7) ± 0.015 | 5.19(8) ± 0.015 |
| 4 | 38.4 ± 1.0 | 9.88(1) ± 0.010 | 5.21(5) ± 0.010 |
| 5 | 40.0 ± 1.0 | 9.84(6) ± 0.010 | 5.21(8) ± 0.010 |

* Ordered for 240 h at 750° C.

region very close to the Al-rich Nb₂Al phase boundary. Metallographic examination revealed the presence of isolated NbAl₃ precipitates. In this instance also, the now familiar variation in resistance with temperature may be seen.

Table IV lists compositions and lattice parameters for the Ta–Al samples examined. Generally, the data were less reliable in this system due to the presence of more extensive concentration gradients. Fig. 7 shows the temperature–resistance curves for samples 1 and 4 which, although still within the Ta₂Al single phase region, have quite different compositions. Both curves exhibit a similar temperature dependence and are much like those observed for Nb₂Al.

In contrast with the results observed for the V–Co sigma phase [4], the electrical resistance was seen to decrease with decreasing temperature for all compositions examined in both the Nb–Al and Ta–Al systems. The nature of these temperature dependencies may in general be characterized by linear decrease followed by an exponential decrease as very low temperatures are approached. This behaviour parallels that observed for the A-15 material Nb₃Sn [5, 6]. However, the exponential resistance decrease in Nb₃Sn initiates at a higher temperature, near 85 K. Three models have been proposed for this behaviour [5] with one relying on the existence of one-dimensional band structure as proposed by Weger [7]. The band structure of this material results from the presence of transition metal populated, very closely packed, linear atomic chains. Although they form a lower symmetry structure, the Nb₂Al type sigma phases also exhibit this feature. The closely packed chains in the sigma phase exist in the [001] direction and are formed by the E sites (see Fig. 1 and Tables I and II). Transition metal atoms populate the sites forming these chains in both structures. If this structural feature is indeed linked to the resistance controlling mechanism in A-15 phases, a similar mechanism at play in the sigma phase structure may reasonably be anticipated. Owing to the

volatility of Al at the temperatures reached during sigma phase fabrication the samples exhibited small but numerous cracks and pores, precluding reliable direct absolute resistivity measurements. As a result of this, and in the absence of specific heat data, it was not possible to formulate resistance data in the instance.

Fig. 8 is graphical representation of the data listed in Table III. As may be seen from Fig. 8a, there is a rather sharp increase in the resistance ratio as stoichiometry is approached. The peak in this curve is quite symmetrical, as well. This may show the compositionally controlled order dependence of the resistivity changes in this material.

The variation in a_0 with composition (Fig. 8b) indicates a unit cell contraction in these dimensions as the composition shifts toward the Al-rich side of stoichiometry. This variation in a_0 with com-

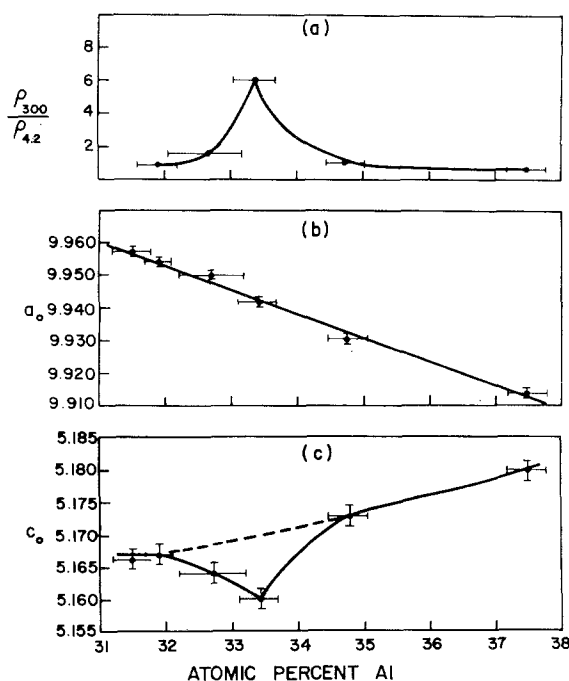


Figure 8 The variation of the resistance ratio (a), the a_0 lattice parameter (b), and the c_0 lattice parameter (c) with composition across the Nb₂Al phase region.

in these systems, however, unless the concomitant c_0 expansion allows the other sites in planes orthogonal to the E site chains to relax inwards.

4. Conclusions

(1) The variation in resistance ratio with composition across the Nb_2Al single phase region exhibiting a sharp peak as stoichiometry is approached, may be viewed as a response to changes in the compositionally dependent order. A c_0 contraction parallels this effect.

(2) Contrary to previously reported behaviour the electrical resistance of Nb_2Al and Ta_2Al was found to decrease with decreasing temperature. The temperature dependence of the decrease exhibits some similarity with that observed in the A-15 structure and may, in general terms, be explained by a band structure similarity.

(3) The decrease in a_0 with increasing Al content across the Nb_2Al and Ta_2Al single phase regions is a result of transition metal replacement. In Ta_2Al there is a change in the rate of contraction at stoichiometry as the A and D sites become completely occupied by Al atoms which then begin to substitute into E and C sites. Similar behaviour could not be observed in Nb_2Al since the Nb-rich phase boundary occurs quite close to stoichiometry.

(4) c_0 remains essentially invariant for Ta_2Al

compositions remote from stoichiometry and to its left since only A and D site substitution is occurring. To the right of stoichiometry, c_0 expands in response to Al substitutions into the E sites in Nb_2Al and Ta_2Al and then into the C sites in Ta_2Al .

Acknowledgements

The authors wish to thank Professor R. W. Boom for his encouragement throughout the course of this work. Thanks are also due Mr R. J. Casper. This work was supported through the University of Wisconsin Inductive Energy Storage Project.

References

1. C. E. LUDIN and A. S. YAMATOTO, *Trans. Met. Soc. AIME* **236** (1966) 863.
2. H. NOWOTNY, C. BRUKL and F. BENESOVSKY, *Monatsch. Chem.* **92** (1961) 116.
3. W. B. PEARSON, "The Crystal Chemistry and Physics of Metals and Alloys" (Interscience, New York, 1972).
4. N. J. MARCONE and J. A. COLL, *Acta Met.* **12** (1964) 742.
5. D. W. WOODARD and G. D. CODY, *RCA Rev.* **25** (1964) 393.
6. R. W. COHEN, G. D. CODY and J. J. HALLORAN, *Phys. Rev. Letters* **19** (1967) 840.
7. M. WEGER, *Rev. Mod. Phys.* **36** (1964) 175.
8. H. P. STUWE, *Trans. Met. Soc. AIME* **215** (1959) 408.

Received 15 January and accepted 15 September 1975.